Eur. Phys. J. E (2016) **39**: 100
DOI 10.1140/epje/i2016-16100-0

THE EUROPEAN
PHYSICAL JOURNAL E

Regular Article

Dynamics of topological monopoles annihilation on a fibre in a thick and thin nematic layer

M. Nikkhou[1], M. Škarabot[1], S. Čopar[2,1], and I. Muševič[1,2,a]

[1] J. Stefan Institute, Jamova 39, SI-1000, Ljubljana, Slovenia
[2] Faculty of Mathematics and Physics, University of Ljubljana, Jadranska 19, SI-1000, Ljubljana, Slovenia

Received 11 July 2016 and Received in final form 29 September 2016
Published online: 26 October 2016 –

Abstract. We study topological defect annihilation on a glass fibre with homeotropic surface anchoring of nematic liquid crystal molecules. The fibre is set parallel to the nematic director of a planar cell with variable thickness and we create pairs of Saturn ring and Saturn anti-ring using the laser tweezers. In thick cells we observe in the whole region of defect separation a Coulomb-like pair attraction with no background force, $F \propto 1/d^{\alpha}$ with $\alpha \approx 2 \pm 0.3$. In cells with thickness comparable to glass fibre diameter, we observe the Coulomb-like attraction only at small separations of the defect pair. For separations larger than the fibre diameter, the pair interaction force is independent of separation. This string-like force is attributed to the formation of defect lines, connecting both monopoles and are indeed visible only on extremely confined fibre, where the fibre diameter is practically equal to the nematic layer thickness. Numerical simulations confirm the formation of defect lines connecting both rings.

1 Introduction

Topological defects [1] are found in regions where the characteristic order of the material is lost. They have attracted much interest due to their importance for understanding frustrated systems, disrupted areas and phase transitions. Topological defects are studied in different branches of physics, from cosmology [2] to condensed matter [3]. In practice, defects interact with each other, which causes their dynamics that affects the macroscopic properties of the system. Their coarsening dynamics and mutual annihilation are therefore of fundamental interest. Liquid crystals (LCs) are condensed matter system, where defects and their dynamics could be studied in real space and real time using optical techniques. They are therefore a test-bed system, where particular theoretical predictions could be tested directly and this allows for extrapolating theory to other areas of physics, where such experiments are difficult or impossible to make. The reason behind this is that LCs are soft, optically anisotropic and transparent and reveal a rich variety of stable and metastable defect structures with appropriate length scales for experimental observations.

Topological defects in LCs [4–6] are singularities of the magnitude of the order parameter, and classified according to their topological charge and winding [7]. The defects are created either by a rapid temperature or pressure quench from the disordered to the ordered state [8,9]. To preserve the conservation of the total topological charge, the disclinations or point defects come in pairs with opposite windings and topological charges. Because of the elastic distortion of the nematic director around the defects, they move toward each other to annihilate, thereby minimizing the elastic energy of the system. In LCs, since the topological defects move within a liquid, the surrounding elastic field changes and, subsequently, the director reorients. The coupling between the changing director field and the velocity field is known as backflow, which has an important effect on the motion of defects [10–16]. The backflow breaks the symmetry of the annihilation dynamics of defects with opposite strength both for $\pm 1/2$ disclinations [16, 17] and ± 1 point defects [14, 18], according to which the positive defect always moves faster than the negative one.

There is a growing body of theoretical and experimental evidence that the interaction between a pair of line or point is modified drastically by confinement. Minoura *et al.* [19] investigated the pair interaction of wedge disclinations with strength of ± 1 in a nematic cell with hybrid alignment. Bogi *et al.* [20] and Yanagimachi *et al.* [17] measured the annihilation dynamics of a dipole of $+1/2$ and $-1/2$ disclination lines in a confined cell with planar surface anchoring, and Dierking *et al.* [14] studied the defect annihilation for ± 1 umbilical defects in a nematic liquid crystal (NLC) with negative dielectric anisotropy, confined in a cell with homeotropic boundary conditions. In the aforementioned studies, the annihilation process is

[a] e-mail: igor.musevic@ijs.si

divided into two regimes depending on the separation between the defects. The cell thickness defines the characteristic length scale, at which the crossing between the two regimes takes place. At separations much larger than the cell (*i.e.* nematic layer) thickness, the defects are connected with characteristic "strings", which results in constant force of attraction and consequently in constant force of mutual approach. These strings are the consequence of the lateral confinement of the system and this regime is dominated by the interaction of liquid crystal with the surfaces. At closer separation and shortly before the annihilation, the elastic energy due to liquid crystal distortion around the defects dominates over the surface anchoring energy. In this near-field regime the annihilation dynamics reflects the true nature of topological defects themselves and is the regime of real interest.

In addition to the creation of defects in temperature or pressure quenches, various topological defects are created when small colloidal particles are immersed in a uniformly aligned NLC. These defects are located in the vicinity of the surfaces of the particles and cannot be separated from the particle or annihilated. They generate forces between colloidal inclusions that could be used for self- or directed assembly of colloidal superstructures [21–33]. It was demonstrated recently that any even number of topological defects in the form of points and strings can be deliberately created on a topologically simple object, such as long, and micrometer-diameter glass fibre with perpendicular surface anchoring of LC molecules [34, 35]. The absorption of the focused beam of laser tweezers was used to locally heat the NLC surrounding the fibre to the isotropic phase. The island of the molten (isotropic) NLC was then rapidly quenched by switching-off the light and a dense tangle of topological defects was immediately created through a process similar to Kibble-Zurek mechanism of defect creation in the early Universe [2,8,36]. During the coarsening time, most of defects annihilated, except those, which were stabilized by the perpendicular alignment of molecules on the fibre. While the controlled creation and annihilation of a pair of rings and monopoles on this fibre has been studied recently in very thick cells (*i.e.* bulk nematic liquid crystal) [18, 34], the effect of confinement on the annihilation dynamics remained rather unexplored.

In this work, we study the effect of confinement on the annihilation dynamics of either a single or multiple pairs of defect rings on a fibre, set parallel to the nematic director in a planar nematic cell. In contrast to previous experiments, where the spacing between the surface of the fibre and the surface of the cell was quite large, in this work the spacing is gradually decreased almost to zero. The rings are created by laser quenching and they appear in a form of a Saturn ring and Saturn anti-ring, encircling the fibre, which is immersed in a thin layer of a NLC. Since the defects are stabilized by a fibre, we can grab an individual ring and separate it from the others by moving it along the fibre using the light of laser tweezers. When both defects are well separated, we quench the region between them and create additional pair of defects. Surprisingly, in very thin cells, these newly created pairs of oppositely charged defects do not attract, but are repelled from each other. Instead of mutually annihilating, they annihilate with the outer pair of defects, which were created first. This puzzling and counter-intuitive behaviour of defects on a fibre is explained by the presence of a tether, connecting both oppositely charged defects on a fibre in very thin cells. This tether has a strong effect on the dynamics of defect annihilation, which is in very thin cells quite different compared to the dynamics in thick cells.

2 Experiment

In our experiments we used glass fibres, a few μm in diameter, which were made by heating of 125 μm optical glass fibres with oxygen-hydrogen torch and mechanical stretching the softened fibre to obtain a desired diameter. The fibres were cleaned and coated with octadecyldimethyl (3-trimethoxysilylpropyl) ammonium chloride (DMOAP silane, ABCR GmbH) to induce very strong homeotropic surface anchoring of nematic liquid crystal 5CB as described in our recent publications [18, 35]. The fibre from the tapered end was sandwiched between two optically transparent ITO coated glass substrates covered by a thin layer of rubbed-polyimide (PI 5291, Brewer Science) to ensure an excellent planar LC orientation. The ITO coating on the inner side of the substrate was providing good control of the local heating of the LC by absorption of the laser light. The Mylar spacers were used to maintain the desired thickness, which was varied from 12 to 70 μm. The cell with Mylar spacers was glued with an epoxy glue (UHU, GmbH or Torr Seal, Varian). The cell thickness was measured by a standard interference technique, using the spectrometer (USB2000, Ocean Optics). Then the fibre was cut from the tapered part with a length of 200–600 μm. The cell was filled with 4′-pentyl-4-cyanobiphenyl (5CB, Nematel) nematic liquid crystal and the micro-fibre was moved inside the cell by capillary force of the LC flow. In the experiments the long axes of the fibres were oriented parallel to the rubbing direction (*i.e.* bulk orientation of the NLC). In some experiments the fibre was placed in a very confined cell as the difference between the diameter of the fibre and the thickness of the cell was only 1–3 μm. Placing the fibre in a very cell with a gap comparable to the fibre diameter is a demanding task due to the fact that the fibre is inserted into the cell by the viscous force of LC flow. To achieve this, we have used a long fibre with both ends of the fibre located outside of the cell.

The laser tweezers setup, which was built around an inverted microscope (Nikon Eclipse, TE2000-U) with an infrared fibre laser operating at 1064 nm, was used as a light source. The deflection of the beam of the tweezers was controlled with a pair of acousto-optic deflectors (AOD) driven by computerized system (Aresis, Tweez 70). The images were recorded using a Pixelink PLA 741 camera at different frame rates from 10 fps to 40 fps.

3 Saturn ring and Saturn anti-ring on a fibre

The fibre with a homeotropic (perpendicular) surface alignment was set parallel to the overall direction of the

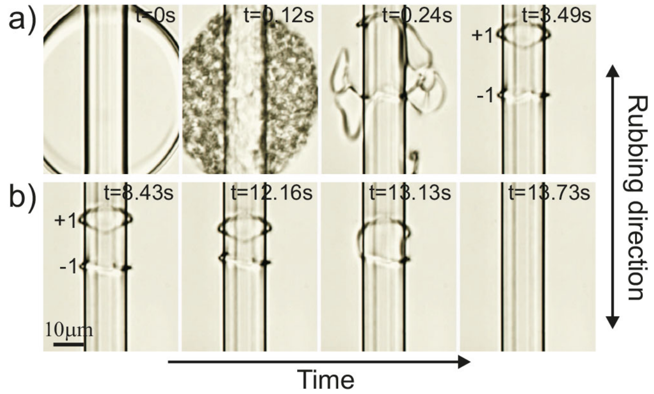

Fig. 1. Creation and annihilation of a pair of topological rings on a fibre set parallel to the nematic director in a planar cell. (a) A pair of Saturn ring and anti-ring are created by thermal quench using a focused laser light. (b) They annihilate into the vacuum if left free.

NLC in cell with planar alignment. Similar to a spherical colloidal particle with homeotropic surface anchoring of LC molecules, a fibre is accompanied by a single hyperbolic hedgehog defect or a Saturn ring, because the genus of the fibre and the micro-sphere are the same and equal to $g = 0$ [37]. The hedgehog is usually located at either end of the fibre, whereas the Saturn ring appears in a form of a small loop, encircling the fibre. This loop can be moved by the tweezers towards an end of the fibre, where it transforms into a point.

The NLC around the fibre far away from the accompanied defect was locally heated into the isotropic phase, as shown in fig. 1(a), creating a molten area with the diameter of tens of μm, using strongly focused laser tweezers beam (several 100 mW). By switching off the light, the isotropic region undergoes a phase transition that leaves behind a dense tangle of defects following the Kibble-Zurek mechanism of topological monopoles formation. In a fraction of a second this tangle annihilates and pins the monopoles on the fibre (see fig. 1(a)). To conserve the total topological charge, the pairs of monopoles with opposite winding number and topological charges were created in each quench. These monopoles are known as the Saturn ring and the Saturn anti-ring and are individually stable and cannot be annihilated. Because of the opposite topological charges of the rings, they are gradually attracted to each other by elastic deformation of NLC and annihilated into the vacuum (fig. 1(b)). The sign of the topological charges of the two rings are opposite and were analysed and determined in our previous work [34].

4 Dynamics of topological monopoles

We perform the experiments in two different confinements using thick and thin LC cells. In thick cells, the fibre with diameter of 8 μm is placed in a cell with a thickness of 65 μm. The rings are initialized at a separation less than 40 μm, and left free to annihilate. In this case the attractive force comes from elastic interaction between the rings and is governed by the Laplace equation [19, 38]. Thus, the attractive force between the rings can be given by the Coulomb law of electric charge interaction, $F \propto 1/d^2$. During the annihilation process the elastic force will be opposed by the Stokes drag force of equal magnitude, which arises from the motion of the rings through a viscous liquid crystal. However, in our experiments we can determine the force only up to a multiplicative constant, because we are unable to measure the viscosity coefficient of each ring and its change during the interaction. On the other hand, we are interested in the separation dependence and eventual power-law behaviour of the interaction force. If we determine the separation dependence of the velocity of the rings from their recorded trajectory, this will be proportional to the separation dependence of the interaction force up to the multiplicative constant. To this aim, the trajectories of the rings were video recorded at a frame rate of 20 fps. The positions of the rings were determined from each recorded frame using a particle-tracking software with a resolution of ± 100 nm.

The positions of the ring and anti-ring are shown in fig. 2(a) as a function of time during pair annihilation. Here, their starting separation is nearly 30 μm. For separations smaller than 15 μm the relative velocity of the two rings shows a power-law dependence on the separation of the rings, $v \propto 1/d^{\alpha}$ with $\alpha \approx 2 \pm 0.3$ (fig. 2(b)). This is observed both in thin and thick cells. If we consider that the viscosity coefficient does not change with separation, the mutual interaction force follows a power-law that is close to the Coulomb law of monopole attraction.

The difference in the dynamics of monopole interaction in thin and thick cells becomes apparent at larger separations, as shown in fig. 2. In a thin cell of thickness 13 μm and fibre diameter of 8 μm, the annihilation dynamics of ring annihilation has two regimes, as shown in fig. 2(b). At closer separation, the interaction force is of the Coulomb type, but at larger separation $> 15\,\mu$m, the rings attract with a constant velocity v_c, indicating a constant force of attraction. This constant force of attraction could be a result of the "strings" connecting both rings, which is a common situation, observed for pairs of oppositely charged topological defects, connected with strings, such as surface boojums in hybrid nematic films [39, 40].

This constant velocity of approach of the rings increases as the cell gap decreases. It seems that tight confinement of the fibre in thin cells increases the elastic distortion per unit length, resulting in stronger interaction force between the two rings. Figure 3(a) shows the constant velocity at large separation ($\approx 50\,\mu$m) *versus* difference between cell gap and the diameter of the fibre, $D_{\text{cell}} - D_{\text{fibre}}$. This velocity drops to zero when this difference is around 10 μm. On the other hand, the ratio of the velocities of both defect rings is independent of the cell gap and is approximately 1.5 ($v_+/v_- \approx 1.5$) as shown in fig. 3(b). It means that the effect of confining surfaces is the same for both defect rings and is therefore independent of the defect ring winding. This speed anisotropy is similar to the previous experiments [14, 16–19].

The upper panel in fig. 3(b) shows the ratio of the velocities *versus* separation of the rings for three different

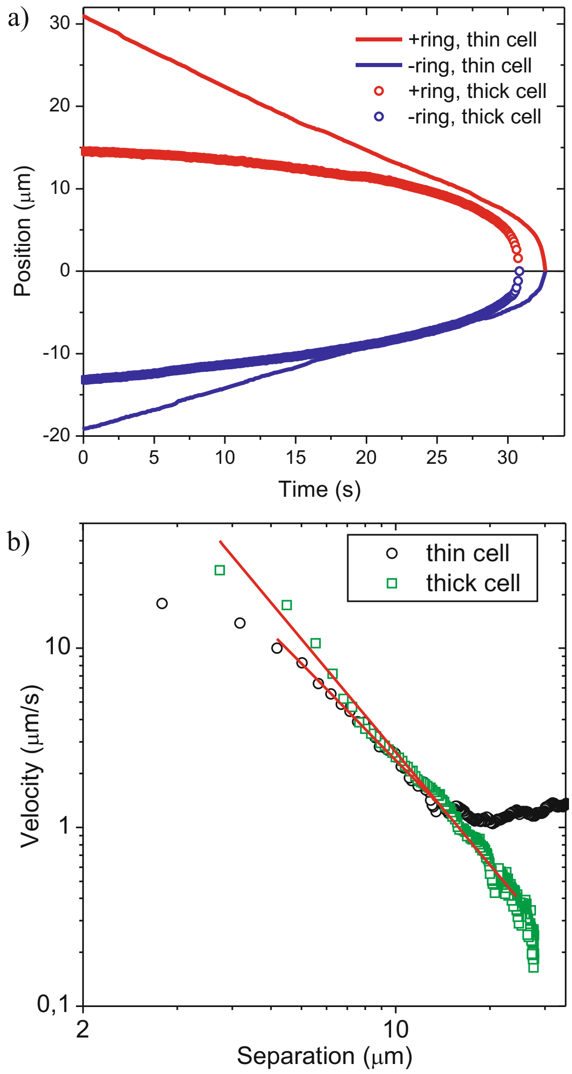

Fig. 2. Annihilation dynamics of a pair of Saturn ring and Saturn anti-ring. (a) The position of the ring and anti-ring *versus* time in thick and thin cells. In thin cells and at larger separation, the ring separation decreases linearly with time. It means that there is a constant attraction force between two rings. (b) The ring relative velocity as a function of their separation in thin and thick nematic cells. In both cases and at small separation, the relative velocity between the rings follows the power-law dependence $v \propto 1/d^{\alpha}$ with $\alpha \approx 2 \pm 0.3$. In this specific experiment in thick cell $\alpha = 2.1$ and in thin cell $\alpha = 1.8$.

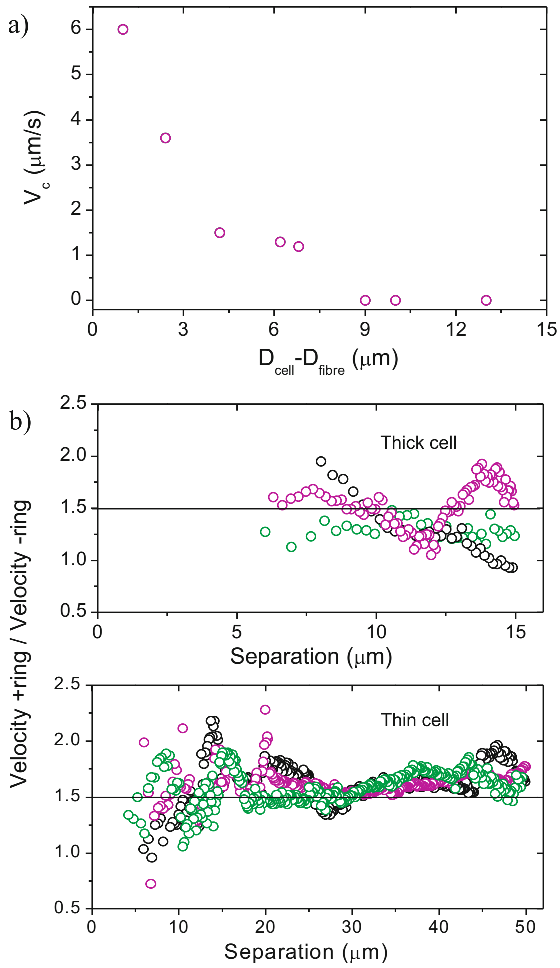

Fig. 3. (a) Constant relative velocity of Saturn ring and anti-ring at large separation *versus* the difference between the cell gap and the fibre diameter. Ratio of the Saturn ring and anti-ring velocities *versus* separation during their annihilation in thick (a) and thin (b) nematic cells for 3 different experiments. This ratio is $v_+/v_- \approx 1.5$.

experiments in thick cells. In this case the data was analyzed when the separation was between 5 and 15 μm. For shorter separations $< 5\,\mu$m the rings join together and create a single ring. For larger separations $> 15\,\mu$m the ratio of the velocity cannot be precisely determined. The surface of the long fibre is not smooth and the impurities and protrusions on the fibre cause friction force for ring dynamics. At larger separations the attraction force between the two rings with opposite charge is very reduced, and this random friction force affects the rings dynamic and the velocity of the rings is uncontrollable and erratic.

For thin cells, the ratio of the velocities is illustrated in the lower panel in fig. 3(b) for three different experiments. Contrary to the thick cells, in thin cells the rings are attracted to each other already from very large separations. In case the fibre is without impurities and protrusions, the rings can attract each other at extreme separations of over $> 100\,\mu$m. As we have shown already in such a region the velocity of the rings is constant, which indicates constant interaction force.

There is therefore a clear indication from the annihilation experiments in thin cells that the rings are connected by some kind of a string-like line, which influences the rings interaction by generating constant force of attraction. In these experiments we can not see directly any connecting defect lines, but we can see their indirect effect, as will be explained in the continuation. The laser light is focused in the vicinity of the fibre with a pair of a ring and anti-ring, as shown in fig. 4(a). The power of the tweezers is increased to heat locally a small area and

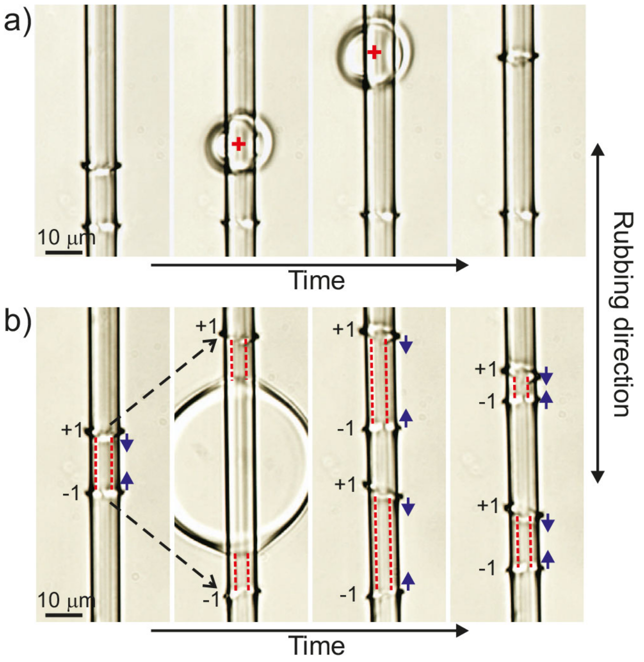

Fig. 4. Defect rings manipulation and interaction in thin cells. (a) Defect ring can be moved along the fibre using the light of laser tweezers. The red crosses indicate the focus of the laser tweezers. (b) By quenching the NLC surrounding the fibre with diameter of 8 μm in a cell with thickness 13 μm a pair of rings is created. These rings are attracted to each other. The rings are separated by laser tweezers and by quenching the region between them another pair of defect rings is created. The connection between the rings is broken and two new connections are established, which are pulling the outer pair of rings together.

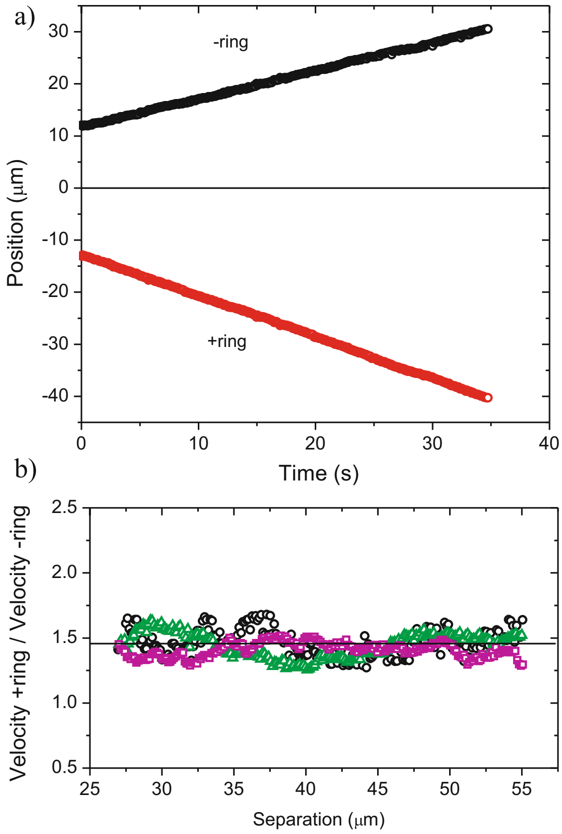

Fig. 5. Dynamics of rings in thin cells. (a) The position of two inner rings created between the initial rings *versus* time. (b) The positive ring moves faster than the negative one and the ratio is $v_+/v_- \approx 1.5$.

create an isotropic island of the liquid crystal, which can strongly attract the defect rings. We can grab and move the ring along the fibre as shown in fig. 4(a).

Using this method, the two rings can be separated to a larger distance, as shown in the last panel of fig. 4(a). Then the fibre is quenched in the middle of these two rings as shown in fig. 4(b). The two new rings are created in between the two outer rings and we expect that these two newly created rings would attract each other. However, this does not happen, because there is an attraction between the two outer rings, as can be seen clearly in the third and fourth panel of fig. 4(b). The quench evidently breaks the line connection between the first two rings and, as a result, new connections are established between the two outer pairs of the rings (panel 3).

Figure 5(a) shows the position of the new created rings *versus* time in the thin cell. These two inner rings are moving away from each other, since the pulling force subjected to the outer rings is stronger than the elastic interaction force between two oppositely charged topological rings. Their velocities are constant and the ratio is $v_+/v_- \approx 1.5$ for three different experiments (see fig. 5(b)).

The "strings" which are obviously connecting the outer pair of rings in thin cells are difficult to observe, unless we take a very thin cell, just fitting to the diameter of the fibre. We therefore performed the experiments in very con-

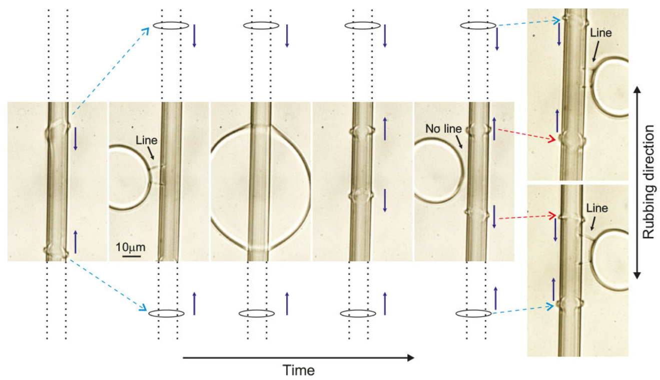

Fig. 6. String-like line between topological rings. A small region of a long fibre with the diameter of 11 μm inside a very confined cell with the thickness of 12 μm is quenched by laser tweezers. A pair of topological rings is created, which are connected by a string-like line. These rings are separated to the far distance and the area between them is quenched. The new pair is created that breaks the string-like line and creates two new string-like lines with outer rings.

fined cell, where the diameter of a fibre is 11 μm and the cell gap is 12 μm. By quenching the NLC surrounding the fibre, a pair of rings were created, which are connected by

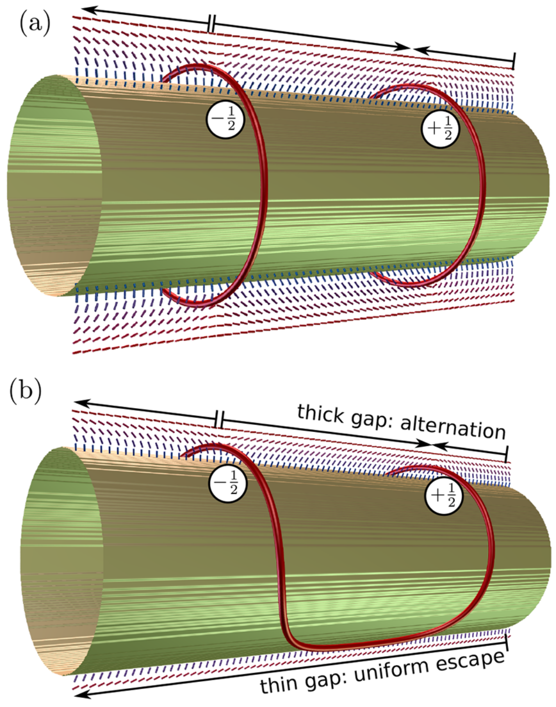

Fig. 7. Numerical simulation of the connected ring structure in thin nematic cells. (a) In thick nematic cells the two rings are separated by a distorted region of the NLC, with no singular lines connecting them. (b) In thin cells, the thin gap between the cell bottom and the fibre discourages defect rings to close on the bottom. Instead, long tethers form, which pull the rings together regardless of their separation. Note that the escape direction in the bottom gap does not alternate like it does on the top. This numerically generated defect structure is not in equilibrium, and collapses, like it was observed in the experiments.

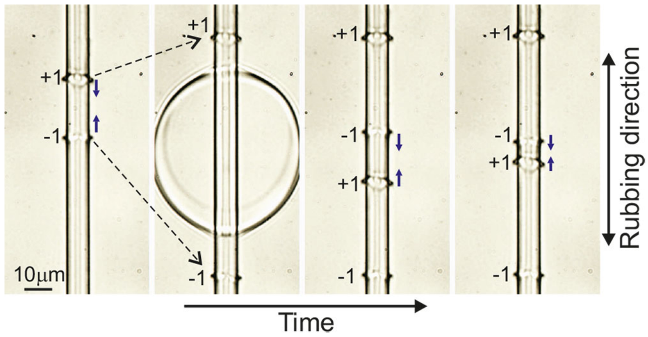

Fig. 8. Creation and annihilation of pairs of rings in a thick cell. Two rings which are created by quenching the NLC around the fibre with diameter of 8 μm in 30 μm cell, are separated by the laser tweezers. The rings are stable because of the large separation between them. By quenching the NLC between these two rings, another pair is created. The rings of the second pair attract each other, as they are closer together.

string-like lines (see fig. 6, first panel). These lines cannot be seen when they are along the fibre, but we can grab them with tweezers as shown in the second panel. The thinner is the cell gap, the stronger is the string-like constant force, leading to fast motion and annihilation of the rings. In the next step, we grabbed the defect rings and moved them to a large separation in order to quench the LC in between them and create new pair of rings (third and fourth panel). The new pair has broken the line connection between the rings of the first pair and created two new connections between the two outer rings. There is no string-like line between the inner rings, since we could not grab it by the laser tweezers (see fifth panel). The line between the outer rings can be seen in the sixth and seventh panel of fig. 6.

To investigate the connected ring structure qualitatively, fibre in a thin cell was modelled using the Landau-de Gennes model on a finite difference grid, using the same scheme and parameters as in ref. [34]. The results are shown in fig. 7(a) for the rings in thick cell and in fig. 7(b) for the thin cell. The simulation shows that when the gap between the fibre and the cell wall is very confined, defects that form during the quench do not extend across the gap, and a long tether forms along both ends of the fibre, connecting the two rings. The "escape" direction from the perpendicular director on the fibre to the planar on the cell wall, alternates between defect rings on top of the fibre, but in the narrow gap below, it remains constant, as shown in fig. 7(b). If the gap is thicker, the tethers either collapse beneath the fibre or slip off on top, but a narrow gap has a stabilizing effect.

By performing a similar experiment in thick cell we achieve totally different results, which are shown in fig. 8. Unlike rings in thin cells, the newly created rings in thick cells behave as expected. Hence, the newly created rings always tend to attract each other, as shown in fig. 8, and they are quite stable at large separations. In this case the effective interaction force is only due to the elastic force between two oppositely charged rings and there is no defect line connecting them and giving rise to a constant, string-like attraction.

5 Conclusions

This work demonstrates the strong influence of the confinement on the dynamics of ring-like monopole annihilation on a fibre. When the fibre is set parallel to the nematic director in a planar cell, one is able to create an arbitrary even number of monopoles. These appear in a form of the Saturn ring and the Saturn anti-ring, having opposite winding numbers and topological charge. When a single pair is created by the laser quenching of the NLC around the fibre, the monopoles are always attracted towards each other and annihilated into the vacuum. However, in thin cells, these two rings are connected with a pair of line defects, which provide a constant, string-like force of attraction of this pair. If an additional pair is created in between, these line defects are cut and reconnected to the newly formed pair of rings. This results in an unusual repulsion of the oppositely charged inner pair of rings and attraction between the oppositely charged outer pair of rings. This does not happen in thick cells, where the pair interaction is fundamentally different and exhibits only the Coulomb-like attraction.

This work was supported by the European Commission Marie Curie project HIERARCHY grant PITN-GA-2008-215851 (M. N.), the Slovenian Research Agency (ARRS) contracts P1-0099 and J1-6723 (I. M., M. Š.), and Z1-6725 (S. Č.).

References

1. N. Mermin, Rev. Mod. Phys. **51**, 591 (1979).
2. T.W.B. Kibble, J. Phys. A **9**, 1387 (1976).
3. P.M. Chaikin, T.C. Lubensky, *Principles of Condensed Matter Physics* (Cambridge University Press, Cambridge, 1995).
4. M.V. Kurik, O.D. Lavrentovich, Sov. Phys. Usp. **154**, 381 (1988).
5. M. Kleman, O.D. Lavrentovich, *Soft Matter Physics* (Springer-Verlag, Berlin, 2003).
6. G.P. Alexander, B.G. Chen, E.A. Matsumoto, R.D. Kamien, Rev. Mod. Phys. **84**, 497 (2012).
7. S. Čopar, Phys. Rep. **538**, 1 (2014).
8. I. Chuang, R. Durrer, N. Turok, B. Yurke, Science **251**, 1336 (1991).
9. M.J. Bowick, L. Chandar, E.A. Schiff, A.M. Srivasava, Science **263**, 943 (1994).
10. G. Toth, C. Denniston, J.M. Yeomans, Phys. Rev. Lett. **88**, 105504 (2002).
11. D. Svenšek, S. Žumer, Phys. Rev. E **66**, 021712 (2002).
12. C. Liu, J. Shen, X. Yang, Commun. Comput. Phys. **2**, 1184 (2007).
13. G. Toth, C. Denniston, J.M. Yeomans, Phys. Rev. E **67**, 051705 (2003).
14. I. Dierking, M. Ravnik, E. Lark, J. Healey, G.P. Alexander, J.M. Yeomans, Phys. Rev. E **85**, 021703 (2012).
15. P. Oswald, J. Igneś-Mullol, Phys. Rev. Lett. **95**, 027801 (2005).
16. C. Blanc, D. Svenšek, S. Žumer, M. Nobili, Phys. Rev. Lett. **95**, 097802 (2005).
17. T. Yanagimachi, S. Yasuzuka, Y. Yamamura, K. Saito, J. Phys. Soc. Jpn. **81**, 034601 (2012).
18. M. Nikkhou, M. Škarabot, I. Muševič, Phys. Rev. E **93**, 062703 (2016).
19. K. Minoura, Y. Kimura, K. Ito, R. Hayakawa, Phys. Rev. E **58**, 643 (1997).
20. A. Bogi, P. Martinot-Laharde, I. Dozov, M. Nobili, Phys. Rev. Lett. **89**, 225501 (2002).
21. P. Poulin, D.A. Weitz, Phys. Rev. E **57**, 626 (1998).
22. R. Pratibha, N.V. Madhusudana, Mol. Cryst. Liq. Cryst. **178**, 167 (1990).
23. Y. Gu, N.L. Abbott, Phys. Rev. Lett. **85**, 4719 (2000).
24. I. Muševič, M. Škarabot, U. Tkalec, M. Ravnik, S. Žumer, Science **313**, 954 (2006).
25. M. Škarabot, M. Ravnik, S. Žumer, U. Tkalec, I. Poberaj, D. Babič, N. Osterman, I. Muševič, Phys. Rev. E **76**, 051406 (2007).
26. M. Škarabot, M. Ravnik, S. Žumer, U. Tkalec, I. Poberaj, D. Babič, N. Osterman, I. Muševič, Phys. Rev. E **77**, 031705 (2008).
27. A.B. Nych, U.M. Ognysta, V.M. Pergamenshchik, B.I. Lev, V.G. Nazarenko, I. Muševič, M. Škarabot, O.D. Lavrentovich, Phys. Rev. Lett. **98**, 057801 (2007).
28. I. Muševič, M. Škarabot, Soft Matter **4**, 195 (2008).
29. U. Ognysta, A. Nych, V. Nazarenko, I. Muševič, M. Škarabot, M. Ravnik, S. Žumer, I. Poberaj, D. Babič, Phys. Rev. Lett. **100**, 17803 (2008).
30. A. Nych, U. Ognysta, M. Škarabot, M. Ravnik, S. Žumer, I. Muševič, Nat. Commun. **4**, 1489 (2013).
31. M. Ravnik, M. Škarabot, S. Žumer, U. Tkalec, I. Poberaj, D. Babič, N. Osterman, I. Muševič, Phys. Rev. Lett. **99**, 247801 (2007).
32. B. Senyuk, Q. Liu, S. He, R.D. Kamien, R.B. Kusner, T.C. Lubensky, I.I. Smalyukh, Nature **493**, 200 (2013).
33. B. Senyuk, M.B. Pandey, Q. Liu, M. Tasinkevych, I.I. Smalyukh, Soft Matter **493**, 200 (2015).
34. M. Nikkhou, M. Škarabot, S. Čopar, M. Ravnik, S. Žumer, I. Muševič, Nat. Phys. **11**, 183 (2015).
35. M. Nikkhou, M. Škarabot, I. Muševič, Eur. Phys. J. E **38**, 23 (2015).
36. W.H. Zurek, Phys. Rep. **276**, 177 (1996).
37. O.D. Lavrentovich, Liq. Cryst. **24**, 117 (1998).
38. B. Yurke, A.N. Pargellis, T. Kovacs, D.A. Huse, Phys. Rev. E **47**, 1525 (1993).
39. O.D. Lavrentovich, S.S. Rozhkov, JETP Lett. **47**, 254 (1988).
40. A. Rapini, L. Leger, A. Martinet, J. Phys. (Paris) Colloq. **36**, C1-189 (1989).